Self-Organized Porphyrin Dimer as a Highly Specific Receptor for Pyrazine Derivatives

Yasuhisa Kuroda,*,† Ayato Kawashima, Yuichirou Hayashi, and Hisanobu Ogoshi*

Contribution from the Department of Polymer Science, Kyoto Institute of Technology, Sakyo-ku, Matsugasaki, Kyoto 606, Japan, and Department of Synthetic Chemistry and Biological Chemistry, Kyoto University, Sakyo-ku, Kyoto 606, Japan

Received October 29, 1996[⊗]

Abstract: Complex formation between pyrazine derivatives and dimeric self-assembly of αααα-isomer of *meso*-tetrakis(2-carboxy-4-nonylphenyl)porphyrin Zn complex (**1·Zn**) was investigated. Thermal atropisomerization of **1·Zn** in a nonpolar solvent such as toluene gives the αααα-atropisomer exclusively. Vapor pressure osmometry for the resultant αααα-atropisomer solubilized in $CHCl_3$ shows molecular weight of 2650 ± 200, indicating formation of dimeric self-assembly of **1·Zn**. ^{1}H NMR and UV/vis titration experiments for this dimeric assembly with pyrazine derivatives show highly specific 1:2 complex formation of pyrazine and **1·Zn**. The equilibrium constants for **1·Zn** dimer/pyrazine complex formation are estimated to be over 10^7 M^{-1}. The most characteristic feature of the present ternary system, $(\mathbf{1\cdot Zn})_2$·pyrazine, is that the pyrazine derivative, having a large side moiety such as benzoyl group, can coordinate two zinc atoms inside the dimer cavity by sticking the side moiety out of a window formed between hydrogen-bond pillars of the complex.

Introduction

It is of current interest to construct large-scale three-dimensional chemical structures by using noncovalent interactions which give the systems abilities of reversible self-assembling.[1] Self-assembling abilities in such systems sometimes play an essential role from a viewpoint of not only reversibility but also molecular design of the system, because the abilities make it possible to construct highly complicated structures which are difficult to prepare by usual synthetic procedures. Another advantage of assemblies is that relatively weak interactions used in these self-assembling systems may provide flexibility to perform dynamic processes such as catalytic activities and allosteric conformational changes. We have recently found a self-assembling system consisted of *meso*-tetrakis(2-carboxy-4-nonylphenyl)porphyrin (**1**, Figure 1).[2] This porphyrin showed strongly solvent-dependent atropisomerization and performs self-induced conformational change to give a carcerand-like porphyrin dimer assembly in nonpolar solvents.[3] This assembly has a characteristic inner space available to incorporate and/or coordinate another organic molecule as a third component of the assembly.

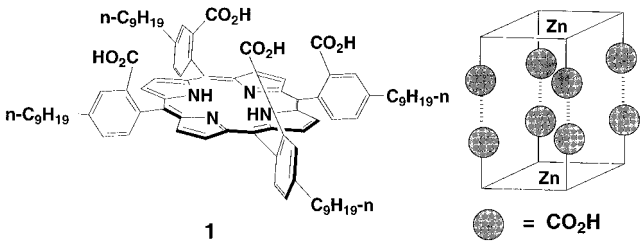

Figure 1. *meso*-Tetrakis(2-carboxy-4-nonylphenyl)porphyrin (**1**) and the schematic structure of the dimer of **1·Zn**.

Here, we report highly specific ternary complex formation between the dimeric zinc/porphyrin assembly and bidentate pyrazine derivatives. The results indicate that the present porphyrin assembly has window-like open sides which are available for binding of a pyrazine derivative bearing a large side chain moiety.

Results and Discussion

Dimeric Assembly of Porphyrin. The zinc complex of **1** (**1·Zn**) shows similar atropisomerization behavior with that of free **1** reported previously[2] and exclusively gives the αααα-atropisomer on thermal isomerization in a nonpolar solvent such as toluene for 4 days as shown in Figure 2a. Vapor pressure osmometry (VPO) for the resultant αααα-atropisomer solubilized in $CHCl_3$ shows molecular weight of 2650 ± 200, which is in good agreement with the dimer of **1·Zn** (MW 1358). Theoretical curve-fitting analyses[2] for this atropisomerization reveal that the observed data in Figure 2a show excellent agreement with the kinetic model which, in addition to the

* Author to whom correspondence should be addressed.

† Kyoto Institute of Technology.

⊗ Abstract published in *Advance ACS Abstracts,* May 1, 1997.

(1) (a) Whitesides, G. M.; Mathias, J. P.; Seto, C. T. *Science* **1991**, *254*, 1312. (b) Dick, D. L.; Rao, T. V. S.; Sukumaran, D.; Lawrence, D. S. *J. Am. Chem. Soc.* **1992**, *114*, 2664. (c) Lehn, J. M. *Science* **1993**, *260*, 1762. (d) Benniston, A. C.; Harriman, A.; Lynch, V. M. *Tetrahedron Lett.* **1994**, *35*, 1473. (e) Anderson, H. L.; Anderson, S.; Sanders, J. K. M. *J. Chem. Soc., Perkin Trans. 1* **1995**, 2231. (f) Goodman, M. S.; Jubian, V.; Linton, B.; Hamilton, A. D. *J. Am. Chem. Soc.* **1995**, *117*, 11610. (g) Valdes, C.; Spitz, U. P.; Toledo, L. M.; Kubik, S. W.; Rebek, J., Jr. *J. Am. Chem. Soc.* **1995**, *117*, 12733. (h) Mathias, J. P.; Seto, C. T.; Simanek, E. E.; Whitesides, G. M. *J. Am. Chem. Soc.* **1994**, *116*, 1725. (i) Collin, J. P.; Harriman, A.; Heitz, V.; Odobel, F.; Sauvage, J. P. *J. Am. Chem. Soc.* **1994**, *116*, 5679. (j) Chernook, A. V.; Shulga, A. M.; Zenkevich, E. I.; Rempel, U.; Borczyskowski, C. V. *J. Phys. Chem.* **1996**, *100*, 1918. (k) Fujita, M.; Nagao, S.; Ogura, K. *J. Am. Chem. Soc.* **1995**, *117*, 1649. (l) Robert, G.; Sherman, J. C. *J. Am. Chem. Soc.* **1995**, *117*, 9081.

(2) (a) Kuroda, Y.; Kawashima, A.; Urai, T.; Ogoshi, H. *Tetrahedron Lett.* **1995**, *36*, 8449. (b) Kuroda, Y.; Kawashima, A.; Ogoshi, H. *Chem. Lett.* **1996**, 57.

(3) For other spontaneous dimeric porphyrin formation systems, see: (a) Aoyama, Y.; Kamohara, T.; Yamagishi, A.; Toi, H.; Ogoshi, H. *Tetrahedron Lett.* **1987**, *28*, 2143. (b) Segawa, H.; Takehara, C.; Honda, K.; Shimidzu, T.; Asahi, T.; Mataga. N. *J. Phys. Chem.* **1992**, *96*, 503. (c) Drain, C. M.; Fischer, R.; Nolen, E. G.; Lehn, J. M. *J. Chem. Soc., Chem. Commun.* **1993**, 243. (d) Kobuke, Y.; Miyaji, H. *J. Am. Chem. Soc.* **1994**, *116*, 4111. (e) Hunter, C. A.; Sarson, L. D. *Angew. Chem., Int. Ed. Engl.* **1994**, *33*, 2313. (f) Sessler, J. L.; Wang, B.; Harriman, A. *J. Am. Chem. Soc.* **1995**, *117*, 704.

S0002-7863(96)03764-X CCC: $14.00

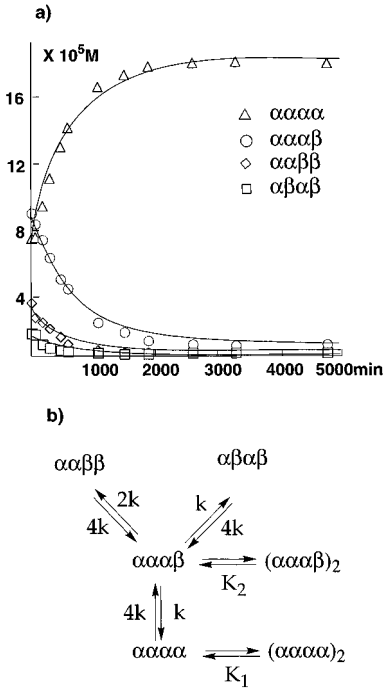

Figure 2. Atropisomerization of **1·Zn**. a) Time courses of thermal atropisomerization of **1·Zn** (2×10^{-4} M) in toluene at 90 °C. Solid lines are theoretical curves obtained by curve fitting analyses using the model shown below of which parameters are $k = 0.0041$ min^{-1}, $K_1 = 2 \times 10^7$ M^{-1}, and $K_2 = 1 \times 10^4$ M^{-1}. b) The kinetic model for atropisomerization of **1·Zn**. The model contains a single rate constant, k, and two equilibrium constants, K_1 and K_2. The rate constant for each isomerization process is statistically weighted. See also ref 2b.

standard model for the atropisomerization of tetraphenylporphyrin (TPP) derivatives as shown in Figure 2b,[4] contains highly efficient dimerization of the αααα-isomer ($K_1 > 10^7$ M^{-1}) and minor one of the ααα*β*-isomer ($K_2 \approx 10\,000$ M^{-1}).

The αααα-isomer also shows characteristic solvent-dependent properties in its electronic and infrared spectra. The Soret band observed at 422 nm in CH_2Cl_2, which is significantly blue-shifted compared with that in THF (431 nm), suggests formation of a face-to-face assembly in CH_2Cl_2.[5] The C═O stretching of the carboxylic acid moieties is found at 1695 cm^{-1} in CH_2Cl_2 and 1728 cm^{-1} in THF. The observed difference agrees well with that between absorptions of monomeric carboxylic acids solvated with ether and dimeric ones.[6] These spectroscopic data, characteristic atropisomerization, and VPO behavior demonstrate face-to-face assembly formation of αααα-**1·Zn** using hydrogen bonds between four pairs of carboxylic acid moieties as shown in Figure 1.

Pyrazine Coordination on Porphyrin Dimer. The molecular model shows that the present porphyrin dimer has an interesting coaxial coordination space of which top and bottom ends are capped with two zinc atoms located within 8 −9 Å distance, which seems to be suitable for incorporation of small bidentate ligand such as pyrazine. The coordination behavior of the assembly is investigated by using various types of ligands shown in Figure 3. Specific complex formation between the

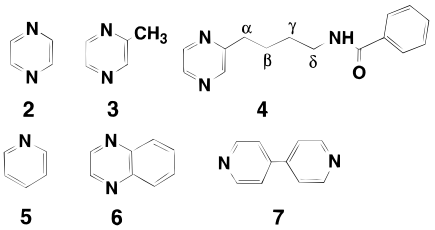

Figure 3. Ligands examined in this work.

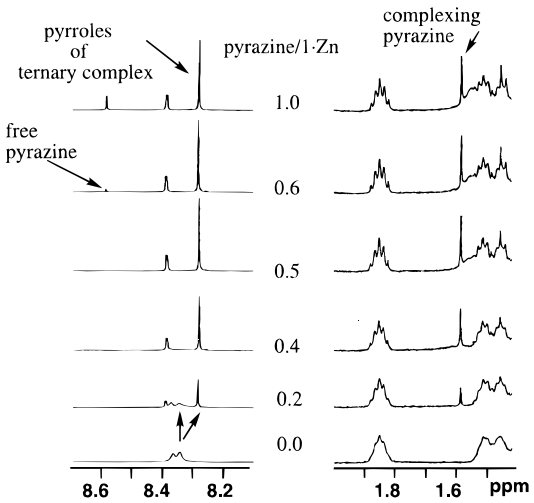

Figure 4. ^{1}H NMR spectra (500 MHz) of **1·Zn** (1 mM) titrated with pyrazine (0−1 mM) in $CDCl_3$ at 25 °C.

1·Zn dimer and pyrazine (**2**) is easily detected by spectroscopic titration using ^{1}H NMR and electronic spectra. The typical NMR titration data are shown in Figure 4. Interestingly both signals due to free and complexing pyrazine and the **1·Zn** dimer can be observed independently in the titration. Pyrrole protons of **1·Zn** appear at δ 8.34 ppm (free) and δ 8.28 ppm (complexed), and pyrazine signals appear at δ 8.59 ppm (free) and δ 1.57 ppm (complexed), respectively.[7] These simple spectroscopic characteristics directly give clear information on stoichiometry of present complexation, i.e., at concentrations of pyrazine less than half an equivalent of **1·Zn**, all pyrazine protons and the **1·Zn** pyrrole protons corresponding to 2 equiv amount of added pyrazine are observed as the complexed form. Increasing the concentration of pyrazine over half an equivalent of **1·Zn**, the signal of free **1·Zn** disappears and the free pyrazine signals appear at 8.59 ppm in addition of complexed one at 1.57 ppm. These observations evidently suggest very strong 2:1 complex formation between **1·Zn** and pyrazine. Further quantitative data on the present complexation are obtained from UV/vis spectroscopic titration shown in Figure 5. Titration of **1·Zn** with pyrazine results in significant red-shift of the Q band absorption, and titration curves obtained from absorption change at 568 nm show a sharp saturation at the concentration ratio of **1·Zn**/pyrazine = 2:1. The titration data clearly indicate specific complex formation between dimeric (**1·Zn**)$_2$ and pyrazine with an equilibrium constant estimated to be greater than 10^7 M^{-1}.[8]

(4) (a) Gottwald, L. K.; Ullman, E. F. *Tetrahedron Lett.* **1969**, 3071. (b) Colleman, J. P.; Gagne, R. R.; Reed, C. A.; Halbert, T. R.; Lang, G.; Robinson, W. T. *J. Am. Chem. Soc.* **1975**, *97*, 1427. (c) Hatano, K.; Anzai, K.; Nishino, A.; Fujii, K. *Bull. Chem. Soc. Jpn.* **1985**, *58*, 3653. (d) Crossley, M. J.; Field, L. D.; Forster, A. J.; Harding, M. M.; Sternhell, S. *J. Am. Chem. Soc.* **1987**, *109*, 341.

(5) (a) Osuka, A.; Maruyama, K. *J. Am. Chem. Soc.* **1988**, *110*, 4454. (b) Collman, J. P.; Bencosme, C. S.; Barnes, C. E.; Miller, B. D. *J. Am. Chem. Soc.* **1983**, *105*, 2704.

(6) Flett, M. St. C. *J. Chem. Soc.* **1951**, 962.

(7) Following examples of large upfield shifts of bidentate ligands sandwiched by porphyrins are reported. (a) For 4,4′-bipyridyl covalently linked face-to-face porphyrin systems, see: Uemori, Y.; Nakatsubo, A.; Imai, H.; Nakagawa, S.; Kyuno, E. *Inorg. Chem.* **1992**, *31*, 5164. (b) For pyrazine polymeric porphyrin systems, see: Marvaud, V.; Launay, J. P. *Inorg. Chem.* **1993**, *32*, 1376.

(8) Since the titration curves are almost linear, indicating the very large K_3 value, the curve-fitting analyses, in spite of excellent agreement between experimental and theoretical curves, results in poor standard deviations (over 50%) for the parameter. Therefore, only the order of magnitude is meaningful.

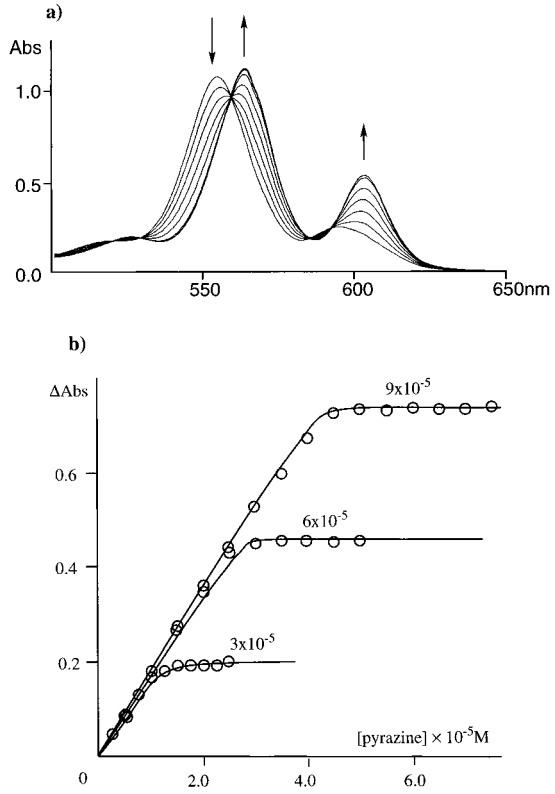

Figure 5. UV/vis spectroscopic titration of **1·Zn** with pyrazine. (a) Spectral change of **1·Zn** on addition of **2** at 25 °C: [**1·Zn**] = 6 × 10^{-5}, [pyrazine] = 0, 4.98, 9.90, 14.8, 19.6, 24.4, 29.1, 33.8, 38.5, 43.1, and 47.6 × 10^{-6} M. (b) Absorption changes at 568 nm observed for titration of **1·Zn** with **2** in CH_2Cl_2 at 25 °C: [**1·Zn**] = 9 × 10^{-5}, 6 × 10^{-5}, and 3 × 10^{-5} M (○, observed points; —, theoretical curves calculated with $K_3 = 2 \times 10^7$ M^{-1}).

$$(\mathbf{1{\cdot}Zn})_2 + \text{pyrazine} \overset{K_3}{\rightleftharpoons} (\mathbf{1{\cdot}Zn})_2{\cdot}\text{pyrazine}$$

In contrast to these results, no appreciable complex formation at the present low concentration range is observed for any other porphyrin/ligand combination such as **1·Zn**/monodentate ligand (**5**) and the bulky bidentate ligands **6** and **7**, or tetramethyl ester of **1·Zn**/pyrazine. Although these systems show only negligibly small spectral changes at the present low concentration range of the ligands (<2 × 10^{-5} M), they form the usual 1:1 complex at much higher ligand concentrations (>5 × 10^{-4} M). The titration data for **6** is shown in Figure 6 as a typical example of such weak complex formation. The titration curves show slow saturation at the high concentration range of the ligand, and usual curve-fitting analyses gives the association constant of 2.3 × 10^2 M^{-1}.[9] The association constants for **1·Zn**/**5**, **1·Zn**/**7**, and the tetramethyl ester of **1·Zn**/pyrazine are similarly determined to be 6.5 × 10^2, 1.3 × 10^3, and 1.9 × 10^3 M^{-1}, respectively. Thus, the distinctive behavior of **1·Zn**/pyrazine system clearly indicates that pyrazine molecule is incorporated into the cavity of the **1·Zn** dimer to coordinate two zinc atoms coaxially.

In order to extend the applicability of the present highly specific self-assembling system, the ligand 2-methylpyrazine was examined and found to act similarly as a specific ligand for the present 2:1 complex formation with **1·Zn**. This

(9) Although simple complex formation, **1·Zn** + L ⇌ **1·Zn**·L, is assumed for analyses of these systems, the systems may contain further equilibrium processes to form other complexes such as (**1·Zn**)$_2$·L and L·(**1·Zn**)$_2$·L, where the ligands coordinate on Zn from outside of the dimer. These equilibrium processes, however, could not be separated by the present titration analyses.

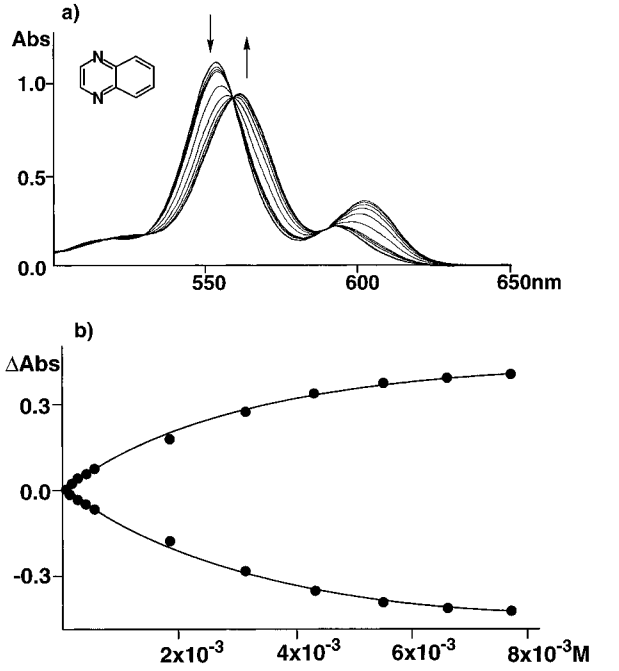

Figure 6. UV/vis spectroscopic titration of **1·Zn** with **6**. (a) Spectral change of **1·Zn** on addition of **6** at 25 °C in CH_2Cl_2: [**1·Zn**] = 6 × 10^{-5} M. (b) Titration curves. Solid lines are theoretical curves obtained by curve-fitting analyses using 1:1 complex formation with $K = 2.3 \times 10^2$ M^{-1}.

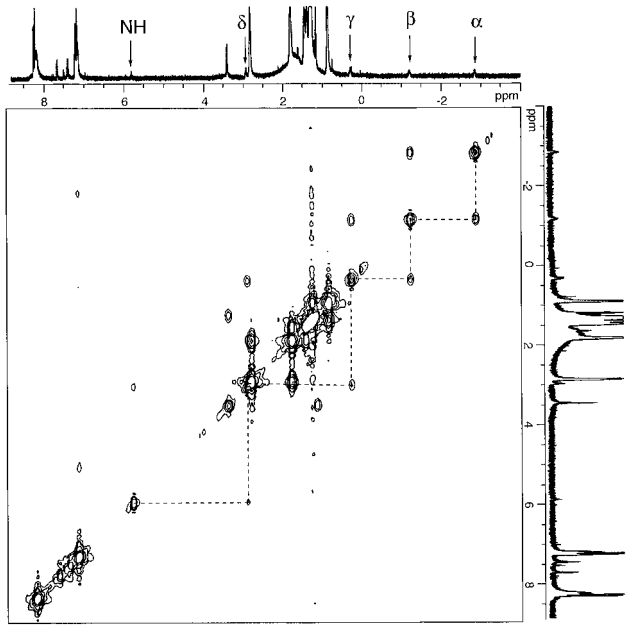

Figure 7. The COSY spectrum (500 MHz) of the assembly consisted of **1·Zn** (1 mM) and pyrazine derivative **4** (0.5 mM) in $CDCl_3$ at 25 °C.

observation is noteworthy, because it suggests that the alkyl substitution at the 2-position of pyrazine does not hinder present coordination severely. We attempted to take advantage of this observation for the purpose of construction of a further new type of self-assembling system by using a newly designed ligand (**4**). In spite of its side chain which is evidently too large for the inner space of the **1·Zn** dimer, the UV/vis spectroscopic titration experiments of **1·Zn** with **4** show normal 2:1 complex formation with $K_3 \approx 10^7$ M^{-1}. This interesting situation is clarified by examination of ^{1}H COSY spectrum of the 1:2 mixture of **1·Zn** and **4**, shown in Figure 7. Although detailed analyses of the spectrum are still incomplete due to line

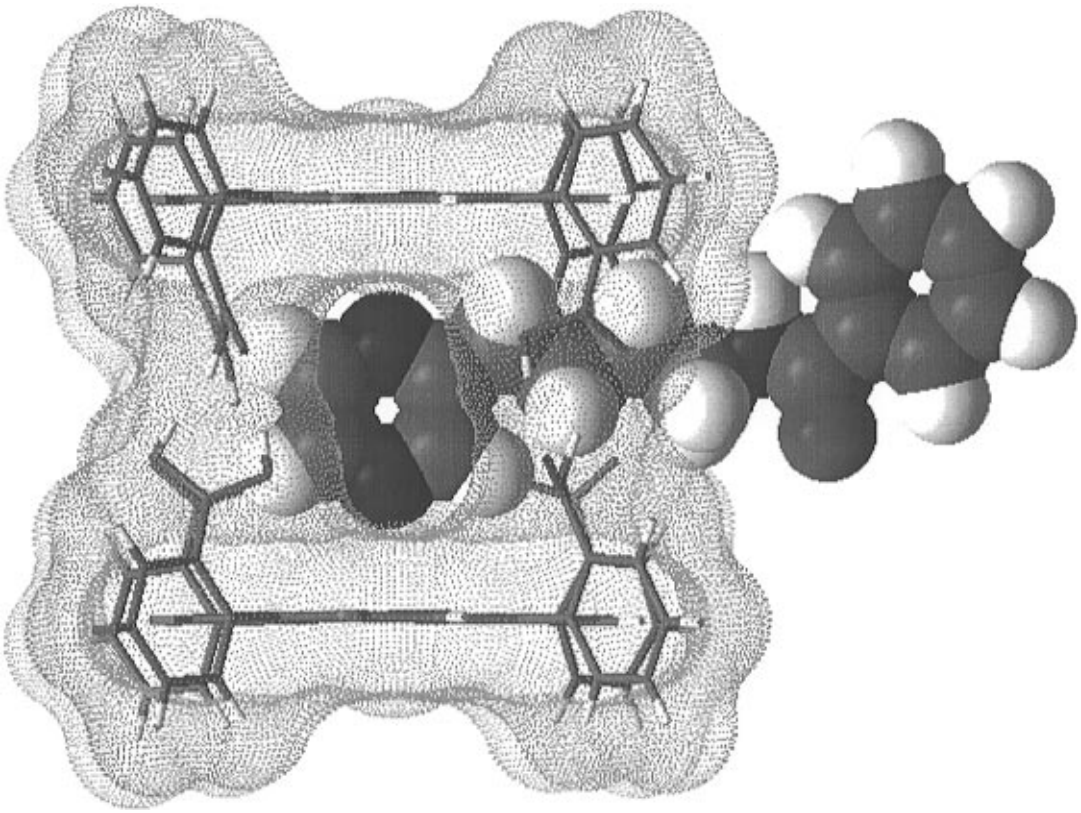

Figure 8. A schematic structure of the assembly (**1·Zn**)$_2$·**4**. The figure is generated with NMRGRAPH, Molecular Simulations Inc., and dots show the solvent accessible surfaces of (**1·Zn**)$_2$.

broadening and the lack of symmetry, characteristic upfield shifts of the side chain of **4** on complexation are obvious, i.e., α, *β*, *γ*, *δ*, and amide protons of **4** (see Figure 3) originally observed at 2.88, 1.88, 1.70, 3.52, and 6.32 ppm shift to −2.84, −1.19, 0.32, 2.98, and 5.87 ppm, respectively. The benzoyl protons of **4**, however, show no significant shifts and appear at the normal aromatic region (*δ* 7.49, 7.58, and 7.75 ppm) even in the complexed form. These observations are fully consistent with the unique structure of the present complex (**1·Zn**)$_2$·**4**, shown in Figure 8, where the pyrazine moiety coordinates two zinc atoms extending the methylene side chain along the surface of porphyrins and the benzoyl moiety is stuck out of a window formed between hydrogen-bond pillars of the complex.

The present complex may provide not only a porphyrin dimer which have unique "inside−outside" connection but also a basic component for larger-scale self-assemblies which consist of several other assemblies connected to each other.

Conclusion

The present results illustrate an interesting example of self-assembling systems which provide unique chemical structures by relatively simple procedures. From the viewpoint of synthetic chemistry, the great advantage of the self-assembling system is that even if many intermediate compounds are involved, the reversibility of each compound forming step allows the system to settle into a thermodynamically most stable assembly. Since it is rationally expected that variety of functional groups may be appended to the pyrazine moiety without changing the core structure of the present assembly, we are now trying to apply the assembly to systems having further functions such as energy and/or charge transfer.

Experimental Section

General Methods. ^{1}H NMR spectra were recorded on a JEOL α-500 (500 MHz). Electronic absorption spectra were performed on a multichannel photodiode array spectrometer (Hewlett-Packard HP-8452A), thermostated at given temperatures with a circulation system (Neslab Instruments, Inc. RTE-9). IR spectra were recorded on Perkin-Elmer System2000 FT-IR. Vapor pressure osmometory measurement was performed on Corona 117. Mass spectra were obtained with a JEOL JMS DX-300 or a JEOL JMS-SX102A mass spectrometer. HPLC experiments were performed on a Waters M600E equipped with a Waters M991 photodiode array detector.

Materials. The solvent used in spectral measurement was Spectrosol purchased from Nacalai Tesque, Inc., or Dojindo Laboratories. Other commercially available chemicals were purchased from Wako Pure Chemical Industries, Ltd., Nacalai Tesque, Inc., or Tokyo Kasei Kogyo Co., Ltd., and employed without further purification, unless stated otherwise.

Kinetic Measurement of Atropisomerization of 1·Zn. A solution of porphyrin (2×10^{-4} M) was placed in a test tube with a stir bar under N_2 atmosphere in a thermostated bath. For the analyses, the concentration of each atropisomer was determined periodically in aliquots (50 *μ*L) sampled from the reaction mixture. The sample was diluted to 500 *μ*L with DMSO and esterified by diazomethane ether solution. After the excess of diazomethane was removed in vacuo and a small amount of water was added, the sample was extracted with ether. This extract was concentrated and injected into HPLC (column YMC, A-813 C4, eluent, methanol/water = 100:1.8, detected at 420 nm, flow rate = 1 mL/min). Retention time of each atropisomer of [*meso*-tetrakis(2-(methoxycarbonyl)-4-nonylphenyl)porphyrinato]-zinc(II): *αβαβ* = 15.5 min, *ααββ* = 16.5 min, *αααβ* = 18.5 min, *αααα* = 39.0 min. Kinetic analyses are carried out as described previously.[2b]

Molecular Weight Determination by Vapor Pressure Osmometry. Molecular weight determinations were performed with a Corona 117 vapor pressure osmometer operated at 40 °C. The molecular weights of the complexes were measured in concentration from 2 to 16 mM. At each concentration, 3 or 4 measurements were repeated. Calibration curves were prepared using polystyrene (MW 2500, polydispersity 1.09) as a molecular weight standard.

Specific Procedures. [*meso*-Tetrakis(2-carboxy-4-nonylphenyl)-porphyrinato]zinc(II) (1·Zn). To the solution of *meso*-tetrakis(2-

carboxy-4-nonylphenyl)porphyrin (100 mg, 0.077 mmol) in chloroform (8 mL) was added a saturated solution of zinc acetate in methanol (3 mL). After a few minutes of stirring and checking by UV/vis spectrophotometry, the mixture is treated with 1M HCl (10 mL), washed with water several times, dried over Na_2SO_4, and concentrated in vacuo. Recrystallization from CH_2Cl_2/hexane gave 78 mg of **1·Zn** as a purple solid (75%). For the αααα atropisomer: ^{1}H NMR (500 MHz, THF-d_8) δ 8.56 (s, 8H), 8.25 (d, J = 1.8 Hz, 4H), 7.85 (d, J = 7.5 Hz, 4H), 7.58 (dd, J = 7.5, 1.8 Hz, 4H), 2.99 (t, J = 7.8 Hz, 8H), 1.95 (m, 8H), 1.6−1.3 (several peaks, 48H), 0.92 (t, J = 7.0 Hz, 12H); ^{1}H NMR (500 MHz, CD_2Cl_2) δ 8.39 (d, J = 2.0 Hz, 4H), 8.29 (s, 8H), 7.31 (dd, J = 7.5, 2.0 Hz, 4H), 7.06 (d, J = 7.5 Hz, 4H), 2.91 (t, J = 7.5 Hz, 8H), 1.86 (m, 8H), 1.6−1.3 (several peaks, 48H), 0.91 (t, J = 7.0 Hz, 12H); FAB MS (*m*-nitrobenzyl alcohol matrix) 1359 $(M + H)^+$; UV/vis (in CH_2Cl_2) λ_{max} (log ϵ, concentration) 422 nm (5.58, 5×10^{-6}), 555 nm (4.23, 3×10^{-5}), 600 nm (3.67, 3×10^{-5}); UV/vis (in THF) λ_{max} (log ϵ, concentration) 431 nm (5.73, 5×10^{-6}), 563 nm (4.33, 3×10^{-5}), 604 nm (4.01, 3×10^{-5}); IR (in CH_2Cl_2) ν_{CO} 1695 cm^{-1}; IR (in THF) ν_{CO} 1728 cm^{-1}. Anal. Calcd for ($C_{84}H_{100}N_4O_8Zn + H_2O$): C, 73.26; H, 7.48; N, 4.07. Found: C, 73.19; H, 7.40; N, 4.02.

4-(2-Pyrazinyl)-*N*-benzoylbutanamide (4). A solution of 100 mg (0.43 mmol) of *N*-(5,6-diaminohexyl)benzamide[10] in 1 M KOH MeOH (1 mL) was stirred at 0 °C in an ice bath, and a solution of 121 mg (0.43 mmol) glyoxal sodium hydrogen sulfite monohydrate in H_2O (1 mL) was added. The solution was allowed to warm to room temperature and stirred overnight. Air was bubbled through the solution for 3 h. The reaction mixture was extracted with ethyl acetate, and the organic layer was dried over Na_2SO_4 and evaporated under reduced pressure to yield 22 mg of **4** as a white solid (20%): ^{1}H NMR ($CDCl_3$) δ 8.48 (s, 2H, pyrazine), 8.41 (d, 1H, pyrazine), 7.76 (d, 2H, phenyl), 7.49 (t, 1H, phenyl), 7.43 (t, 2H, phenyl), 6.32 (s, 1H, amide), 3.52 (q, 2H, CH_2), 2.88 (t, 2H, CH_2), 1.88 (m, 2H, CH_2), 1.70 (m, 2H, CH_2); FAB MS (*m*-nitrobenzyl alcohol matrix) 256 $(M + H)^+$.

JA963764G

(10) Cox, J. P. L.; Craig, A. S.; Helps, I. M.; Jankowski, K. J.; Parker, D.; Eaton, M. A. W.; Millican, A. T.; Millar, K.; Beeley, N. R. A.; Boyce, B. A. *J. Chem. Soc., Perkin Trans. 1* **1990**, 2567.